Jestr

Journal of Engineering Science and Technology Review 15 (2) (2022) 117 - 126

Research Article

JOURNAL OF
Engineering Science and Technology Review

www.jestr.org

Theoretical Back Analysis of Internal Forces of Primary Support in Shallow Tunnels Subjected to Eccentric Loads

Wenzheng He[1,*] and Jing He[2]

[1]*School of Urban Construction Engineering, Chongqing Open University, Chongqing 401520, China*
[2]*Department of Mathematics and Science, Chongqing College of Mobile Communication, Chongqing 401520, China*

Received 19 February 2022; Accepted 1 June 2022

Abstract

The geology and topography of shallow tunnels subjected to eccentric loads is asymmetric. Compared with deep tunnels, shallow tunnels have a supporting structure characterized by a more complex stress state. Moreover, because of the uncertainty of parameters of the surrounding rock and the field construction conditions in tunnels, the stress state of the primary support cannot be accurately evaluated through theoretical analysis and numerical simulation. To accurately analyze the stress state of primary support of the shallow tunnels subjected to eccentric loads, this study proposed a novel back-analysis method to evaluate the internal forces of primary support by measuring radial displacement and contact stress. According to the stress characteristics of primary support, the primary support was regarded as a circular curved beam, and the theory of circular curved beam was used to deduce the analytical solutions of these internal forces. A case study was conducted to analyze the internal forces of the primary support obtained using the proposed method. Combined with the monitoring data of the tunnel, the internal force of the primary support was inverted, and the difference between the deep-buried side and the shallow-buried side was analyzed. Results show that the internal force distribution of the primary support of the shallow-bias tunnels is obviously asymmetric, and the internal force of the deep-buried side is larger than that of the shallow-buried side. This study provides a significant reference for the dynamic design and optimization of construction for primary support in shallow-bias tunnels.

Keywords: Shallow tunnels, Eccentric loads, Primary support, Back analysis

1. Introduction

The terrain of the central and western regions of China is complex, and tunnels account for a large proportion of traffic structures. Because of terrain or geological factors, loads on the two sides of the supporting structure are asymmetric in the portal section of the tunnels, and shallow tunnels subjected to eccentric loads are formed. Compared with deep tunnels, shallow tunnels subjected to eccentric loads have a more complicated stress state, and the possibility of accidents is higher. Therefore, accurate calculation of the stress state of the support is important to determine a structural design and construction scheme of shallow tunnels subjected to eccentric loads.

However, due to the asymmetric geology and topography of shallow-bias tunnels, the surrounding rock load on their supporting structure is significantly different from that of deep tunnels [1-2]. In addition, uncertain surrounding rock parameters and site construction conditions during tunnel construction result in extremely complex mechanical responses of the surrounding rock and supporting structure during tunnel construction. Because of the asymmetry of stress and the uncertainty of surrounding rock parameters, analyzing the stress state of the supporting structure of shallow tunnels by theoretical calculation or numerical simulation is difficult. Therefore, the back analysis method is an effective means to evaluate the safety of tunnel construction [3-4]. However, accurately calculating the internal forces of the primary support by using monitoring data remains a problem and demands prompt solutions.

Scholars have conducted numerous studies on the back analysis method in geotechnical engineering [5-8]. However, most of the existing studies on this method take the mechanical parameters of rock mass as the inversion target, and there is no means to directly analyze the internal forces of the support structure in the tunnel. Research on the back analysis theory of the primary support of shallow tunnels subjected to eccentric loads is scarce. Therefore, an urgent problem to be solved is how to accurately invert the internal force of the primary support in shallow tunnels subjected to eccentric loads by using the monitoring data.

This study extensively analyzed the stress characteristics of shallow tunnels subjected to eccentric loads. The analytic expressions for the internal forces of primary support were deduced by using the theory of circular curved beam, and the internal force distribution characteristics of the primary support of shallow tunnels subjected to eccentric loads were analyzed to quickly evaluate the stress states of the primary support. This study provides references for the dynamic design and optimization of construction in tunnel engineering.

2. State of the art

Numerous studies have been conducted on monitoring measurements and back analysis of underground structures. With elastic modulus, cohesive forces and friction angle of the foundation as the inversion target, An et al. [9] proposed a back analysis method based on stress and displacement for

*E-mail address: hewenzheng1982@126.com
ISSN: 1791-2377
doi:10.25103/jestr.152.15

segment-lined tunnels. This method analyzed the stability of mechanically excavated tunnels, but cannot directly analyze the stress state of the lining structure. Houda et al. [10] proposed a 3D numerical back analysis method for soft soil under quasi-static vertical cyclic loading, and compared the back analysis results with the experimental results obtained on a 3D small-scale model. Applying the theory of similarity and linear elasticity equations, Niu et al. [11] took the surrounding rock pressure as the back analysis target and established a back analysis method that combines model test and numerical simulation. However, the internal forces under the back-calculation load still deviates from the measured value in different degrees. Combining optimization algorithm and 3D model, Miranda et al. [12] proposed an inversion algorithm of geotechnical mechanical parameters. Janin et al. [13] investigated the complex 3D effect of the interaction of excavation process, reinforcement, tunnel support load, and foundation reaction force by using a numerical inversion method in simulation. Tarifard et al. [14] established a direct back analysis model based on displacement, and studied the creep characteristics of rock and the influence of groundwater on the long-term stability of tunnels. However, this model cannot describe the stress of tunnels under unsymmetrical pressure. Wang et al. [15] proposed an intelligent back analysis method based on IA-BP algorithm, and developed the corresponding intelligent back analysis program to study the creep characteristics of rock mass under stress-seepage coupling. This model is applicable to the back analysis of multi-field coupling parameters. Lee et al. [16] put forward a back analysis model of rock load of multi-arch tunnel with cracks based on stress variable method, calculated the rock load caused by cracks during excavation, and determined the relationship between load strength and deformation modulus of rock mass. However, this model cannot evaluate the stress state of shallow tunnel lining. Mahmoudi et al. [17] developed a univariate back analysis model based on the finite difference method, and inverted the rock and soil parameters according to the displacement values obtained from tunnel monitoring. The results show that the rock and soil parameters extracted by back analysis have high accuracy in tunnel design. Yu et al. [18] established a deformation parameter inversion model for relaxed columnar jointed rock mass based on displacement monitoring data. Relaxation factor was introduced to describe the deterioration degree of parameters of relaxed columnar jointed rock mass. The model was verified by the acoustic detection results. An et al. [19] developed a back analysis method based on a variety of monitoring information by using differential evolution algorithm, which can accommodate multiple target variables such as elastic modulus of foundation, friction angle, and elastic modulus of concrete lining for back analysis. In addition, the algorithm can also use monitoring data, such as displacement and stress, to evaluate the elastic modulus of concrete lining and the performance of reinforced foundation. Ghorbani et al. [20] optimized the geomechanical parameters of an underground hydropower station cavern in Lavarak, Iran by using continuous ant colony algorithm and multivariate regression. According to the calculation results, the error value of the continuous ant colony algorithm is lower than that of multivariate regression. Compared with multivariate regression the continuous ant colony algorithm performs calculation more accurately to obtain the optimal value.

The aforementioned results were mainly obtained from the back analysis of the mechanical parameters of rocks. However, limited studies have been conducted directly on the back analysis of the stress characteristics of the primary support. The back analysis method of the internal force of tunnel support structure based on the elastic foundation beam theory provides a new way to evaluate the mechanical properties of tunnel support. Wang et al. [21] presented an inverse analysis method of the internal force of the primary support in the horseshoe tunnel based on the elastic foundation beam theory. Chen et al. [22] proposed an inversion calculation method of the internal forces of support structures in multi-arc tunnels. The aforementioned two back analysis studies of mechanical properties of primary support based on elastic foundation beam method eliminate the dependence on the overlying surrounding rock, and can quickly reverse the stress of the non-biased tunnel through contact stress, which effectively improves the calculation efficiency. However, the calculation assumption is different from the actual stress of the tunnel, and the calculation method derived from this assumption leads to an obvious error. He et al. [23] revised the internal force inversion model and established an internal force inversion model of the primary support based on radial displacement and contact stress, which is more in line with the actual stress state of the tunnel. However, this theory is only applicable to deep non-biased tunnels.

The above results focus on the inversion of geotechnical mechanical parameters. Research on the inversion analysis of the internal force of the supporting structure, especially the stress of the supporting structure of the shallow tunnels subjected to eccentric loads is scarce. This study analyzed the stress characteristics of the primary support in shallow tunnels subjected to eccentric loads. The internal force inversion formulas of the primary support structure in the detachment zone and the elastic resistance zone were derived according to the theory of circular curved beam. Moreover, the internal force distributions of the primary support were discussed. The proposed method can quickly evaluate the internal force state of primary support of the shallow-bias tunnel to provide a reference for the optimization of the primary support design and construction in tunnels.

The rest of this study is organized as follows: Section 3 establishes a mechanical model and proposes the back-analysis method for the internal force of primary support in shallow tunnels subjected to eccentric loads. Section 4 discusses the applicability of the method through case studies. Finally, section 5 summarizes this study and draws relevant conclusions.

3. Methodology

3.1 Governing differential equation

Detachment and resistance zones exist in support structures of mountain tunnels. The former bears only active load, while the latter bears both active load and passive loads (Fig. 1). The contact stress between the surrounding rock and the support structure is composed of passive and active loads. The existing inverse model of internal force of primary support derived from the elastic foundation beam theory does not consider the influence of active load [21-22], and its calculation assumption obviously deviates from the actual stress state of the support structure. In [23], this method was modified such that the stress mode of the modified support structure was closer to the real state. This study further deduced the back-analysis method of the internal forces of primary support in shallow-bias tunnel considering the asymmetry of topography and geology.

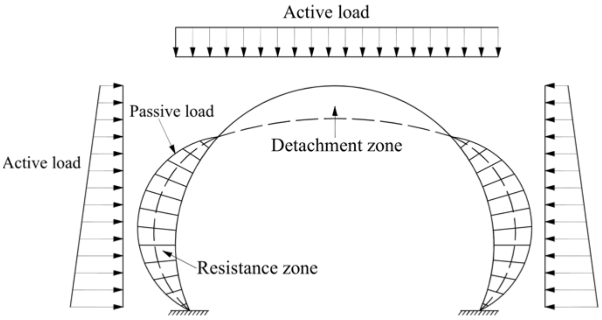

Fig. 1. Load of supporting structure

The cross section of a highway tunnel is generally a multi-centered circle, and its primary support can be viewed as a circular curved beam. The geometric shape of the primary support is shown in Fig. 2. The stress diagram of micro unit $rd\theta$ is shown in Fig. 3, where K is the coefficient of the elastic resistance of surrounding rocks, $\omega(\theta)$ is the radial displacement, $\omega(\theta)$ takes the circle center direction as the positive direction, and $\delta(\omega)=\begin{cases}1 & \omega<0\\ 0 & \omega\geq 0\end{cases}$.

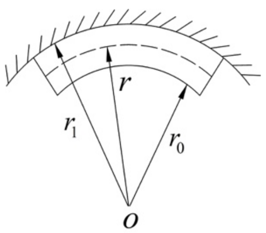

Fig. 2. Geometric shape of primary support

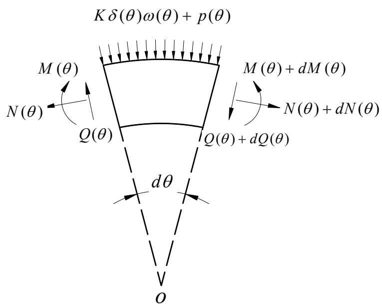

Fig. 3. Stress sketch of micro unit

According to the stress balance condition of the micro unit and the relationship between the radial displacement of curved beam and internal force [23], the fifth-order ordinary differential equation can be derived as follows:

$$\frac{d^5\omega(\theta)}{d\theta^5}+2\frac{d^3\omega(\theta)}{d\theta^3}+m^2\frac{d\omega(\theta)}{d\theta}=F\frac{dp(\theta)}{d\theta} \tag{1}$$

where $p(\theta)$ is the radial force generated by active load, $m^2=1-KF\delta(\omega)$, $F=-\frac{(r^3A+rI)r_1}{EIA}$, A is the cross-section area, and I is the inertia moment.

Generally, the combined support of steel arch and shotcrete is adopted for the primary support of highway tunnels (Fig. 4). E is the equivalent elastic modulus and I is the equivalent moment of inertia of the cross section. E and I can be solved as follows:

$$\begin{cases}EI=E_sI_s+E_cI_c\\ EA=E_sA_s+E_cA_c\end{cases} \tag{2}$$

where E_s is the elastic modulus of the steel arch, E_c is the elastic modulus of shotcrete, I_s is the moment of inertia of the steel arch, I_c is the moment of inertia of shotcrete, A_s is the cross-sectional area of the steel arch, and A_c is the cross-sectional area of shotcrete.

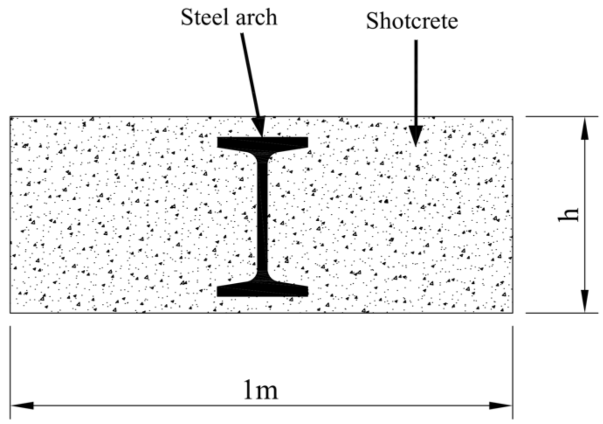

Fig. 4. Combined support of steel arch and shotcrete

The contact stress between the surrounding rock and support of the shallow-bias tunnel is radial stress, which can be calculated by vertical pressure and lateral pressure of the surrounding rock (Fig. 5). The contact stress can be expressed as follows:

$$p(\theta)=\overline{p}_v\cos(\theta)+\overline{p}_h\sin(\theta) \tag{3}$$

where $\overline{p}_v$ is the vertical pressure and $\overline{p}_h$ is the lateral pressure.

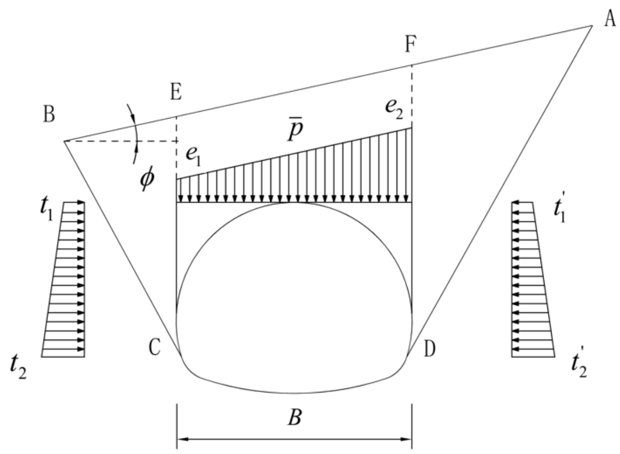

Fig. 5. Surrounding rock pressure in shallow-bias tunnel

$\overline{p}_v$ and $\overline{p}_h$ can be expressed as follows:

$$\begin{cases}\overline{p}_v=\overline{p}+\zeta r_1\sin\theta\\ \overline{p}_h=\lambda\left[\overline{p}+r_1\gamma\left(1-\cos\theta\right)\right]\end{cases} \tag{4}$$

Substitution of Eq. (4) into Eq. (3) leads to the following equation:

$$p(\theta)=\left(\lambda\bar{p}+\lambda r\gamma\right)\sin\theta+\bar{p}\cos\theta+\frac{1}{2}\left(\zeta r_1-\lambda r_1\gamma\right)\sin 2\theta \tag{5}$$

where ζ is the slope of vertical load, $\zeta=\tan(\varphi)\gamma$, φ is the slope angle of the ground, $\bar{p}$ is the vertical pressure of the vault, and γ is the weight of surrounding rock. The section where the vertical axis of the tunnel lies is utilized as the initial section where $\theta=0$. The clockwise direction is positive and the counterclockwise direction is negative. λ is the lateral pressure coefficient, and its sign is related to θ. If θ is positive, then it takes the positive sign. If θ is negative, then it takes the negative sign.

For shallow-bias tunnels, the lateral pressure coefficients of the deep-buried side and shallow-buried side are different. $\bar{p}$ and λ can be calculated from the measured contact stress. Let $Q=\lambda\bar{p}+\lambda r_1\gamma$ and $U=\zeta r_1-\lambda r_1\gamma$, and the following equations can be obtained:

$$p(\theta)=Q\sin\theta+\bar{p}\cos\theta+\frac{1}{2}U\sin 2\theta \tag{6}$$

$$\frac{dp(\theta)}{d\theta}=Q\cos\theta-\bar{p}\sin\theta+U\cos 2\theta \tag{7}$$

The following five-order ordinary radial displacement differential equation can be derived by substituting Eq. (7) into Eq. (1):

$$\frac{d^5\omega(\theta)}{d\theta^5}+2\frac{d^3\omega(\theta)}{d\theta^3}+m^2\frac{d\omega(\theta)}{d\theta}=-F\bar{p}\sin\theta+FQ\cos\theta+FU\cos 2\theta \tag{8}$$

In the detachment zone, the elastic resistance of the surrounding rocks is neglected. Thus, $\delta(\omega)=0$, and Eq. (8) can be written as:

$$\frac{d^5\omega(\theta)}{d\theta^5}+2\frac{d^3\omega(\theta)}{d\theta^3}+\frac{d\omega(\theta)}{d\theta}=-F\bar{p}\sin\theta+FQ\cos\theta+FU\cos 2\theta \tag{9}$$

3.2 Solution of governing differential equation

Governing differential equation is solved in two cases.

3.2.1 Solution of governing differential equation considering elastic resistance

In the resistance zone, $\delta(\omega)=1$. The governing equation of the curved beam is the fifth-order non-homogeneous differential equation with constant coefficients (Eq. (8)), and its complete solution ($\omega(\theta)$) is the sum of general solution ($\omega_0(\theta)$) of the homogeneous differential equation and the special solution ($\omega^*(\theta)$) of the non-homogeneous differential equation, as follows:

$$\omega(\theta)=\omega_0(\theta)+\omega^*(\theta) \tag{10}$$

According to the theory of differential equations, the general solution of homogeneous differential equation can be expressed as follows:

$$\omega_0(\theta)=C_1+C_2 ch\alpha\theta\cos\beta\theta+C_3 sh\alpha\theta\cos\beta\theta+C_4 ch\alpha\theta\sin\beta\theta+C_5 sh\alpha\theta\sin\beta\theta \tag{11}$$

where $\alpha=\sqrt{\frac{m-1}{2}}$, $\beta=\sqrt{\frac{m+1}{2}}$ and C_1 - C_5 are integration constants. The special solution of non-homogeneous differential equation can be calculated by constant variation method:

$$\omega^*(\theta)=\frac{FQ}{\left(m^2-1\right)}\sin\theta+\frac{F\bar{p}}{\left(m^2-1\right)}\cos\theta+\frac{FU}{\left(16+2m^2\right)}\sin 2\theta \tag{12}$$

Substituting Eqs. (11) and (12) into Eq. (10), we can obtain the complete solution of the governing differential equation:

$$\omega(\theta)=C_1+C_2 ch\alpha\theta\cos\beta\theta+C_3 sh\alpha\theta\cos\beta\theta+C_4 ch\alpha\theta\sin\beta\theta+C_5 sh\alpha\theta\sin\beta\theta+\frac{FQ}{\left(m^2-1\right)}\sin\theta+\frac{F\bar{p}}{\left(m^2-1\right)}\cos\theta+\frac{FU}{\left(16+2m^2\right)}\sin 2\theta \tag{13}$$

3.2.2 Solution of governing differential equation without considering elastic resistance

When the support is located in the detachment zone, it only bears the active load. $\delta(\omega)=0$, thus, $m^2=1$, and the general solution of the governing equation is as follows:

$$\omega_0(\theta)=C_1+C_2\sin\theta+C_3\cos\theta+C_4\theta\sin\theta+C_5\theta\cos\theta \tag{14}$$

Similarly, the constant variation method can be used to obtain the special solution of the non-homogeneous differential equation as follows:

$$\omega^*(\theta)=\frac{F\bar{p}}{8}\left(6\cos\theta+4\theta\sin\theta-\theta^2\cos\theta\right)+\frac{FQ}{8}\left(6\sin\theta-4\theta\cos\theta-\theta^2\sin\theta\right)+\frac{FU}{18}\sin 2\theta \tag{15}$$

The following complete solution can be obtained through Eqs. (14) and (15):

$$\omega(\theta)=C_1+C_2\sin\theta+C_3\cos\theta+C_4\theta\sin\theta+C_5\theta\cos\theta+\frac{F\bar{p}}{8}\left(6\cos\theta+4\theta\sin\theta-\theta^2\cos\theta\right)+\frac{FQ}{8}\left(6\sin\theta-4\theta\cos\theta-\theta^2\sin\theta\right)+\frac{FU}{18}\sin 2\theta \tag{16}$$

3.3 Internal force analysis of primary support

The expressions of the internal forces were deduced in [23]. The shear force, axial force, and bending moment of the support structure are as follows:

$$Q(\theta)=\left(\frac{r^3}{EI}+\frac{r}{EA}\right)^{-1}\left[\frac{d^3\omega(\theta)}{d\theta^3}+\frac{d\omega(\theta)}{d\theta}\right] \tag{17}$$

$$N(\theta)=-\left(\frac{r^3}{EI}+\frac{r}{EA}\right)^{-1}\left[\frac{d^4\omega(\theta)}{d\theta^4}+\frac{d^2\omega(\theta)}{d\theta^2}\right] -Kr_1\delta(\omega)\omega(\theta)-r_1p(\theta) \tag{18}$$

$$M(\theta)=\frac{EI}{r^2}\left\{\frac{d^2\omega(\theta)}{d\theta^2}+\left(\frac{r}{EA}K\delta(\omega)r_1+1\right)\omega(\theta)+\left(\frac{Ar^2}{I}+1\right)^{-1}\left[\frac{d^4\omega(\theta)}{d\theta^4}+\frac{d^2\omega(\theta)}{d\theta^2}\right]+\frac{rr_1}{EA}p(\theta)\right\} \tag{19}$$

3.3.1 Internal force of primary support in resistance zone

In the resistance zone, the expressions of the internal forces can be derived by substituting Eq. (13) into Eqs. (17)-(19) as follows:

$$\begin{aligned}Q(\theta)=T\Big[&\left(C_3A_1-C_4A_2\right)ch\alpha\theta\cos\beta\theta+\\&\left(C_2A_1-C_5A_2\right)sh\alpha\theta\cos\beta\theta+\\&\left(C_2A_2+C_5A_1\right)ch\alpha\theta\sin\beta\theta+\\&\left(C_3A_2+C_4A_1\right)sh\alpha\theta\sin\beta\theta-\\&\frac{6FU}{16+2m^2}\cos2\theta\Big]\end{aligned} \tag{20}$$

where $A_1=\alpha^3-3\alpha\beta^2+\alpha$, $A_2=\beta^3-3\alpha^2\beta-\beta$, and $T=\left(\frac{r^3}{EI}+\frac{r}{EA}\right)^{-1}$.

$$\begin{aligned}N(\theta)=\Big[&\left(-TC_2B_1+TC_5B_2-Kr_1C_2\right)ch\alpha\theta\cos\beta\theta+\\&\left(-TC_3B_1+TC_4B_2-Kr_1C_3\right)sh\alpha\theta\cos\beta\theta+\\&\left(-TC_3B_2-TC_4B_1-Kr_1C_4\right)ch\alpha\theta\sin\beta\theta+\\&\left(-TC_2B_2-TC_5B_1-Kr_1C_5\right)sh\alpha\theta\sin\beta\theta\Big]-\\\Big[&Kr_1C_1+\left(\frac{Kr_1FQ}{m^2-1}+r_1Q\right)\sin\theta+\\&\left(\frac{Kr_1F\overline{p}}{m^2-1}+r_1\overline{p}\right)\cos\theta+\\&\left(\frac{12TFU+Kr_1FU}{16+2m^2}+\frac{1}{2}r_1U\right)\sin2\theta\Big]\end{aligned} \tag{21}$$

where $B_1=\alpha^4-6\alpha^2\beta^2+\beta^4+\alpha^2-\beta^2$, and $B_2=-4\alpha^3\beta+4\alpha\beta^3-2\alpha\beta$.

$$\begin{aligned}M(\theta)=&\\\frac{EI}{r^2}\Big\{\Big[&\left(B_1C_2D-B_2C_5D+C_2E_1-C_5E_2+C_2G\right)ch\alpha\theta\cos\beta\theta+\\&\left(B_1C_3D-B_2C_4D+C_3E_1-C_4E_2+C_3G\right)sh\alpha\theta\cos\beta\theta+\\&\left(B_1C_4D+B_2C_3D+C_4E_1+C_3E_2+C_4G\right)ch\alpha\theta\sin\beta\theta+\\&\left(B_1C_5D+B_2C_2D+C_5E_1+C_2E_2+C_5G\right)sh\alpha\theta\sin\beta\theta\Big]+\\&C_1G+\left(\frac{GFQ-FQ}{m^2-1}+\frac{rr_1Q}{EA}\right)\sin\theta+\\&\left(\frac{GF\overline{p}-F\overline{p}}{m^2-1}+\frac{rr_1\overline{p}}{EA}\right)\cos\theta+\\&\left(\frac{GFU-4FU+12DFU}{16+2m^2}+\frac{rr_1U}{2EA}\right)\sin2\theta\Big\}\end{aligned} \tag{22}$$

where $D=\left(\frac{Ar^2}{I}+1\right)^{-1}$, $G=\left(\frac{r}{EA}Kr_1+1\right)$, $E_1=\alpha^2-\beta^2$, and $E_2=-2\alpha\beta$.

3.3.2 Internal force of primary support in detachment zone

In the detachment zone, without consideration of the elastic resistance of the surrounding rocks, the expressions of the internal forces can be derived by substituting Eq. (16) into Eqs. (17)-(19):

$$\begin{aligned}Q(\theta)=&\left(-2C_4T-\frac{F\overline{p}T}{4}\right)\sin\theta+\left(-2C_5T+\frac{FQT}{4}\right)\cos\theta+\\&\frac{FQT}{2}\theta\sin\theta+\frac{F\overline{p}T}{2}\theta\cos\theta-\frac{FUT}{3}\cos2\theta\end{aligned} \tag{23}$$

$$\begin{aligned}N(\theta)=&\left(-2C_5T-\frac{FQT}{4}-r_1Q\right)\sin\theta+\\&\left(2C_4T-\frac{F\overline{p}T}{4}-r_1\overline{p}\right)\cos\theta+\\&\frac{F\overline{p}T}{2}\theta\sin\theta-\frac{FQT}{2}\theta\cos\theta+\\&\left(-\frac{2FUT}{3}-\frac{1}{2}r_1U\right)\sin2\theta\end{aligned} \tag{24}$$

$$\begin{aligned}M(\theta)=&\frac{EI}{r^2}\{C_1+\\&\left(-2C_5+2C_5D+\frac{3FQ}{4}+\frac{DFQ}{4}+\frac{rr_1Q}{EA}\right)\sin\theta+\\&\left(2C_4+\frac{3F\overline{p}}{4}-2C_4D+\frac{DF\overline{p}}{4}+\frac{rr_1\overline{p}}{EA}\right)\cos\theta+\\&\left(\frac{F\overline{p}}{2}-\frac{DF\overline{p}}{2}\right)\theta\sin\theta+\left(-\frac{FQ}{2}+\frac{DFQ}{2}\right)\theta\cos\theta+\\&\left(-\frac{FU}{6}+\frac{2DFU}{3}+\frac{rr_1U}{2EA}\right)\sin2\theta\Big\}\end{aligned} \tag{25}$$

3.3.3 Expressions of internal forces under symmetrical load

Eqs. (20)-(25) can also be used to solve the internal forces of the primary support in the deep tunnel. Let $\varphi=0$ and $\gamma=0$; thus, $Q=\lambda\overline{p}$ and $U=0$. Considering the symmetry, $C_3=C_4=0$. The preceding conditions are substituted into Eqs.

(20)-(22), and the expressions of the internal forces in the resistance zone can be obtained as follows:

$$Q(\theta)=T\Big[\big(C_2A_1-C_5A_2\big)sh\alpha\theta\cos\beta\theta+ \big(C_2A_2+C_5A_1\big)ch\alpha\theta\sin\beta\theta+\Big] \tag{26}$$

$$N(\theta)=\Big[\big(-TC_2B_1+TC_5B_2-Kr_1C_2\big)ch\alpha\theta\cos\beta\theta+ \big(-TC_2B_2-TC_5B_1-Kr_1C_5\big)sh\alpha\theta\sin\beta\theta\Big]- \left[Kr_1C_1+\left(\frac{Kr_1F\lambda\bar{p}}{m^2-1}+\lambda\bar{p}r_1\right)\sin\theta+\left(\frac{Kr_1F\bar{p}}{m^2-1}+r_1\bar{p}\right)\cos\theta\right] \tag{27}$$

$$M(\theta)= \frac{EI}{r^2}\Big\{\Big[\big(B_1C_2D-B_2C_5D+C_2E_1-C_5E_2+C_2G\big)ch\alpha\theta\cos\beta\theta+ \big(B_1C_5D+B_2C_2D+C_5E_1+C_2E_2+C_5G\big)sh\alpha\theta\sin\beta\theta\Big]+ C_1G+\lambda\bar{p}\left(\frac{GF-F}{m^2-1}+\frac{rr_1}{EA}\right)\sin\theta+ \left(\frac{GF\bar{p}-F\bar{p}}{m^2-1}+\frac{rr_1\bar{p}}{EA}\right)\cos\theta\Big\} \tag{28}$$

$Q=\lambda\bar{p}$ and $U=0$ are substituted to Eqs. (23)-(25). The expressions of the internal forces in the detachment zone can be expressed as follows:

$$Q(\theta)=\left(-2C_4T-\frac{F\bar{p}T}{4}\right)\sin\theta+ \frac{FT\lambda\bar{p}}{4}\cos\theta+\frac{FT\lambda\bar{p}}{2}\theta\sin\theta+\frac{F\bar{p}T}{2}\theta\cos\theta \tag{29}$$

$$N(\theta)=\left(-\frac{FT\lambda\bar{p}}{4}-r_1\lambda\bar{p}\right)\sin\theta+ \left(2C_4T-\frac{F\bar{p}T}{4}-r_1\bar{p}\right)\cos\theta+ \frac{F\bar{p}T}{2}\theta\sin\theta-\frac{FT\lambda\bar{p}}{2}\theta\cos\theta \tag{30}$$

$$M(\theta)=\frac{EI}{r^2}\left\{C_1+\left(\frac{3F\lambda\bar{p}}{4}+\frac{DF\lambda\bar{p}}{4}+\frac{rr_1\lambda\bar{p}}{EA}\right)\sin\theta+ \left(2C_4+\frac{3F\bar{p}}{4}-2C_4D+\frac{DF\bar{p}}{4}+\frac{rr_1\bar{p}}{EA}\right)\cos\theta+ \left(\frac{F\bar{p}}{2}-\frac{DF\bar{p}}{2}\right)\theta\sin\theta+\left(-\frac{F\lambda\bar{p}}{2}+\frac{DF\lambda\bar{p}}{2}\right)\theta\cos\theta\right\} \tag{31}$$

According to (26)-(31), the expressions are completely consistent with that of the deep tunnel in [23], and the expressions of the internal forces of support in shallow tunnels subjected to eccentric loads can degenerate into the formula of the deep tunnel under special conditions. Obviously, the proposed back analysis model has universality.

3.4 Solving integral constants based on measured data

Five displacement data and three contact stress data are used to solve the integral constant. First, $p(\theta)$ in Eq. (3) is obtained through the measured contact stress. Second, $p(\theta)$ is substituted to the radial displacement Eqs. (13) and (16). Five unknown integral constants (C_1 - C_5) can be obtained according to the measured radial displacement data. The layout of the measuring points is presented in Fig. 6.

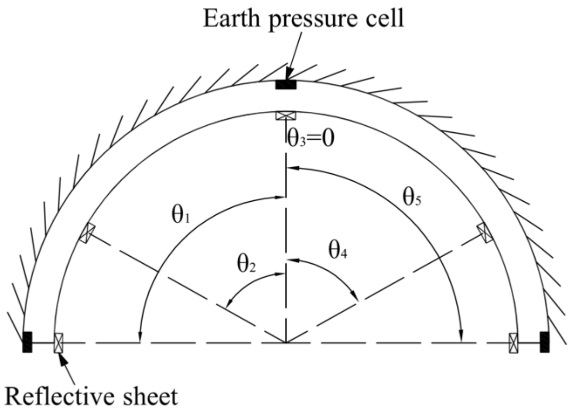

Fig. 6. Layout of displacement and contact stress measuring points

$\bar{p}$ (the contact stress of the vault) can be directly measured. A measurement section is selected in the outer and inner detachment zone, and the section angles are θ_L and θ_R , respectively. The following equations are obtained by substituting the measured contact stress data into Eq. (5):

$$p(\theta_L)=\big(\lambda_L\bar{p}+\lambda_Lr_1\gamma\big)\sin\theta_L+\bar{p}\cos\theta_L+ \frac{1}{2}\big(\zeta r_1-\lambda_Lr_1\gamma\big)\sin 2\theta_L \tag{32}$$

$$p(\theta_R)=\big(\lambda_R\bar{p}+\lambda_Rr_1\gamma\big)\sin\theta_R+\bar{p}\cos\theta_R+ \frac{1}{2}\big(\zeta r_1-\lambda_Rr_1\gamma\big)\sin 2\theta_R \tag{33}$$

According to Eqs. (32) and (33), the lateral pressure coefficientsand of the shallow-buried and deep-buried sides (λ_L and λ_R) can be obtained as:

$$\lambda_L=\frac{p(\theta_L)-\bar{p}\cos\theta_L-\frac{1}{2}\bar{p}\zeta\sin 2\theta_L}{\big(\bar{p}+r_1\gamma\big)\sin\theta_L-\frac{1}{2}r_1\gamma\sin 2\theta_L} \tag{34}$$

$$\lambda_R=\frac{p(\theta_R)-\bar{p}\cos\theta_R-\frac{1}{2}\bar{p}\zeta\sin 2\theta_R}{\big(\bar{p}+r_1\gamma\big)\sin\theta_R-\frac{1}{2}r_1\gamma\sin 2\theta_R} \tag{35}$$

$p(\theta)$ can be derived by substituting Eqs. (34)-(35) into Eq. (5). Currently, the non-contact measurement method has been extensively utilized in monitoring tunnel measurements. The radial displacement can be measured by total station. This method can realize efficient and accurate measurement. The total station can be employed to measure horizontal displacement (Δx) and vertical displacement (Δy) of each measuring point in the cross section. The radial displacement $\omega(\theta)$ and the tangential displacement $\phi(\theta)$ can be obtained by using the rotary formula of the coordinate system (Fig. 7):

$$\phi(\theta)=\Delta x\cos(\theta)+\Delta y\sin(\theta) \tag{36}$$

$$\omega(\theta)=-\Delta x\sin(\theta)+\Delta y\cos(\theta) \tag{37}$$

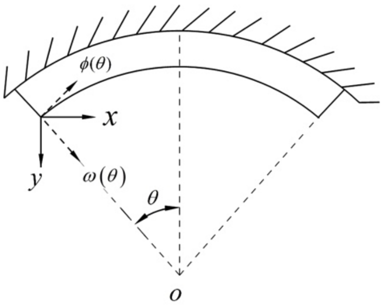

Fig. 7. Transformation of coordinate system

The measured radial displacement data (ω_1 - ω_5) are substituted into the radial displacement solution and the fifth-order linear equations can be obtained, which can be written in matrix form as follows:

$$\begin{bmatrix} 1 & e_1 & f_1 & g_1 & h_1 \\ 1 & e_2 & f_2 & g_2 & h_2 \\ 1 & e_3 & f_3 & g_3 & h_2 \\ 1 & e_4 & f_4 & g_4 & h_3 \\ 1 & e_5 & f_5 & g_5 & h_5 \end{bmatrix} \begin{bmatrix} C_1 \\ C_2 \\ C_3 \\ C_4 \\ C_5 \end{bmatrix} = \begin{bmatrix} J_1 \\ J_2 \\ J_3 \\ J_4 \\ J_5 \end{bmatrix} \tag{38}$$

In the resistance zone, the values of each parameter in Eq. (38) are as follows:

$e_i = ch\alpha\theta_i \cos\beta\theta_i$, $f_i = sh\alpha\theta_i \cos\beta\theta_i$,

$g_i = ch\alpha\theta_i \sin\beta\theta_i$, $h_i = sh\alpha\theta_i \sin\beta\theta_i$, and

$$J_i = \omega(\theta_i) - \frac{F(\lambda\overline{p}+\lambda r_1\gamma)}{m^2-1}\sin\theta_i - \frac{F\overline{p}}{m^2-1}\cos\theta_i - \frac{F(r_1\gamma\tan\varphi - \lambda r_1\gamma)}{16+2m^2}\sin 2\theta_i .$$

In the detachment zone, the lining does not bear the elastic reaction force of the surrounding rock. The parameters in Eq. (38) are as follows:

$e_i = \sin\theta_i$, $f_i = \cos\theta_i$, $g_i = \theta_i \sin\theta_i$, $h_i = \theta_i \cos\theta_i$, and

$$J_i = \omega(\theta_i) - \frac{F\overline{p}}{8}(6\cos\theta + 4\theta\sin\theta - \theta^2\cos\theta) - \frac{F(\lambda\overline{p}+\lambda r_1\gamma)}{8}(6\sin\theta - 4\theta\cos\theta - \theta^2\sin\theta) - \frac{F(r_1\gamma\tan\varphi - \lambda r_1\gamma)}{18}\sin 2\theta .$$

We substitute the measured radial displacement data into Eq. (38) and derive the following expression:

$$\begin{bmatrix} C_1 \\ C_2 \\ C_3 \\ C_4 \\ C_5 \end{bmatrix} = \begin{bmatrix} 1 & e_1 & f_1 & g_1 & h_1 \\ 1 & e_2 & f_2 & g_2 & h_2 \\ 1 & e_3 & f_3 & g_3 & h_2 \\ 1 & e_4 & f_4 & g_4 & h_3 \\ 1 & e_5 & f_5 & g_5 & h_5 \end{bmatrix}^{-1} \begin{bmatrix} J_1 \\ J_2 \\ J_3 \\ J_4 \\ J_5 \end{bmatrix} \tag{39}$$

After solving the integral constant, we can inverse the internal forces of the primary support of the shallow tunnels subjected to eccentric loads by substituting C_1 - C_5 into the analytical expressions of internal forces.

4 Result Analysis and Discussion

The Shizishan tunnel (Fig. 8) is located in Guiyang city, Guizhou province in China. The length of the tunnel is 362 m and the cross section is a three-centered circle. The tunnel was excavated using the step method. The shape of the upper bench is close to a semicircle arch and the central angle of the upper bench is 180°. The primary support of the longitudinal unit length of the tunnel is taken as the calculation object. The geometric parameters of the upper benching section of the primary support are listed in Table 1, and the material parameters are listed in Table 2.

Fig. 8. Photo of the Shizishan Tunnel

Table 1. Geometric parameters of upper bench

Shotcrete thickness $h(m)$	Excavation radius $r_1(m)$	Inner radius $r_0(m)$	cross-sectional area of the steel arch $A_s(mm^2)$
0.20	5.80	5.60	1443

Table 2. Material parameters

Elastic modulus of steel arch $E_T(Gpa)$	Elastic modulus of shotcrete $E_C(Gpa)$	Coefficient of elastic resistance of surrounding rocks $K(Mpa/m)$
206	20	400

K0+060 is the shallow-bias section with a slope angle of 16°. The contact stress is measured by the earth pressure cell (Fig. 9), and the displacement is measured by the total station (Fig. 10). The measured values tend to be stable after 30 days of excavation. The contact stresses between the surrounding rocks and the shotcrete as well as displacement at the measuring points after 30 days of excavation are presented in Tables 3 and 4.

Fig. 9. Earth pressure cell

Fig. 10. Displacement measurement

Table 3. Contact stress

Number of measuring points	$\theta(rad)$	Contact stress $p(Kpa)$
1	-1.571	23.2
2	0	47.5
3	1.571	14.1

Table 4. Vertical and horizontal displacement

Number of measuring points	$\theta(rad)$	$\Delta x(mm)$	$\Delta y(mm)$
1	-1.571	12.6	1.2
2	-1.047	6.4	3.8
3	0.000	-0.2	27.3
4	1.047	-3.9	2.9
5	1.571	-5.2	1.0

The sign of measured radial displacement is positive, indicating that the upper bench of the primary support developed free deformation at this stage. Meanwhile, the surrounding rock has no elastic resistance to the support. Therefore, the internal force of the support structure should be calculated according to Eqs. (23)-(25). The vertical load component and lateral pressure coefficient can be obtained by substituting the data in Table 3 into Eqs. (34)-(35). The data in Table 4 is substituted into Eq. (39) to solve the integral constant. The internal force can be obtained by substituting the integral constant and load parameters into the derived expressions of the internal forces. The internal forces are illustrated in Figs. 11-13.

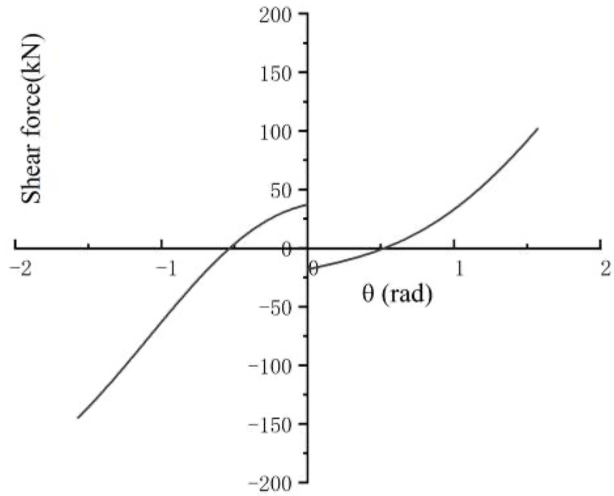

Fig. 11. Shear force of primary support

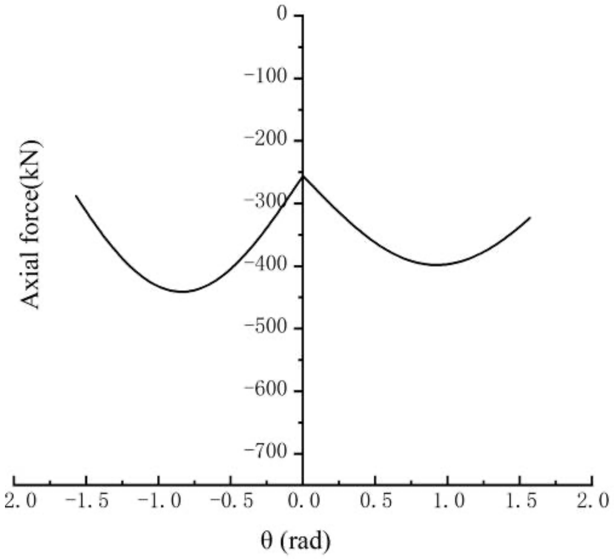

Fig. 12. Axis force of primary support

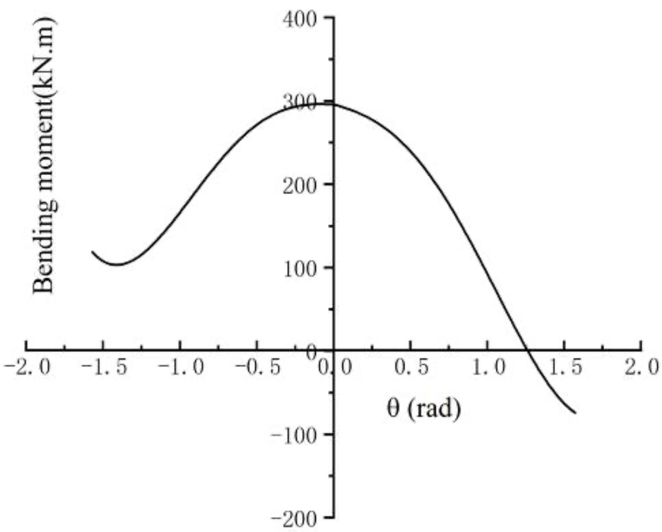

Fig. 13. Bending moment of primary support

Figs. 11-13 show that the internal forces of the deep-buried and shallow-buried sides show obvious asymmetry, and the internal force of the deep-buried side is larger than that of the shallow-buried side. The shear force is positively correlated with the section angle. The maximum shear force is at the arch springing ($\theta=\pi/2$), and the maximum shear force at the deep-buried side is 1.3 times that at the shallow-buried side. During the construction process, the whole section of the primary support is compressed, and the axial force increases first and then decreases with the increase of θ. The axial force reaches the maximum value at $\theta=0.9$. Meanwhile, the vault is the section with the maximum positive bending moment. With the increase of θ, the bending moment gradually decreases, and the shallow-buried side arch springing bears negative bending moment.

5. Conclusions

To evaluate the internal forces accurately, we developed a back-analysis method based on radial displacement and contact stress. This method can be used to estimate the internal forces of the primary support in shallow tunnels subjected to eccentric loads. A case study was conducted to analyze the mechanical characteristics of the primary support obtained using the proposed methods. The following conclusions could be drawn:

(1) The internal forces in the deep-buried side and shallow-buried side are asymmetric. The internal force of the deep-buried side is larger than that of the shallow-buried side. Therefore, the stress state of the shallow tunnels subjected to eccentric loads is more complicated than that of the deep tunnel.

(2) The shear force is positively correlated with the cross-section angle. The shear force at the arch springing is the maximum, while the axial force increases at first and then decreases with the increase of θ. The bending moment is negatively correlated with the cross-section angle and the bending moment of the vault is the maximum.

(3) The vault and arch springing sections of the supporting structure bear large bending moment and axial force, and are prone to cracking and water leakage. Secondary shotcrete can be used to strengthen the support, and the construction of lower benching and inverted arch should be implemented as soon as possible.

Thus, the analytical back-analysis method was proposed to quickly evaluate the internal forces of the primary support in shallow tunnels subjected to eccentric loads. However, due to the lack of onsite monitoring data, future study should modify the model combined with the monitoring data to more accurately understand the stress characteristics of the primary support of tunnels under complex geological conditions.

Acknowledgements
This work was supported by the Natural Science Foundation Project of Chongqing City (Grant Nos. cstc2020jcyj-msxmX0963) and the Scientific and Technological Research Program of Chongqing Municipal Education Commission (Grant Nos. KJQN201904004).

References

1. Du, J. M., Fang, Q., Hai, L., Mai, H. Y., Wang, G., “Calculation method for surrounding rock pressure of shallow tunnel with asymmetrical pressure of variable slopes”. *Journal of Central South University (Science and Technology)*, 52(11), 2021, pp. 4088-4098.
2. Ziaei, A., Ahangari, K., “The effect of topography on stability of shallow tunnels case study: The diversion and conveyance tunnels of Safa Dam”. *Transportation Geotechnics*, 14, 2018, pp. 126-135.
3. Liu, Z. H., Wu, X., “Study on Mechanic Parameters Selection of Rock Slope Based on BP Neural Network Displacement Back Analysis”. *Academic Journal of Engineering and Technology Science*, 4(6), 2021, pp. 31-38.
4. Espada, M., Lamas, L., “Back analysis procedure for identification of anisotropic elastic parameters of overcored rock specimens”. *Rock Mechanics and Rock Engineering*, 50(3), 2017, pp. 513-527.
5. Zhao, H. B., Chen, B. R., Li, S. J., Li, Z., Zhu, C. X., “Updating the models and uncertainty of mechanical parameters for rock tunnels using Bayesian inference”. *Geoscience Frontiers*, 12(5), 2021, pp. 101198.
6. Berti, M., Bertello, L., Bernardi, A. R., Caputo, G., “Back analysis of a large landslide in a flysch rock mass”. *Landslides*, 14(6), 2017, pp. 2041-2058.
7. Srivastav, A., Pandey, V. H. R., Kainthola, A., Singh, P. K., Dangwal, V., Singh, T. N., “Numerical Analysis of a Collapsed Tunnel: A case study from NW Himalaya, India”. *Indian Geotechnical Journal*, 52(1), 2022, pp. 132-144.
8. Öge, İ. F., “Investigation of design parameters of a failed soil slope by back analysis”. *Engineering failure analysis*, 82, 2017, pp. 266-279.
9. An, J. S., Kang, K. N., Choi, J. Y., Sung, W. S., Suy, V., Song, K. I., “Tunnel Back Analysis Based on Differential Evolution Using Stress and Displacement”. *Advances in Civil Engineering*, 2020, 2020, pp. 8156573.
10. Houda, M., Jenck, O., Emeriault, F., “Soft soil improvement by rigid inclusions under vertical cyclic loading: numerical back analysis”. *European Journal of Environmental and Civil Engineering*, 25(3), 2021, pp. 409-428.
11. Niu, H. S., Weng, X. L, Tian, C., Wang, D., Hao, X. J., “Model Test and Back Analysis of Shield Tunnel Load Distribution in Soft Clay”. *Advances in Materials Science and Engineering*, 2021, 2021, pp. 9992348.
12. Miranda, T., Dias, D., Pinheiro, M., Eclaircy-Caudron, S., “Tunnel engineering-influence of the type and the quantity of measurements in the back analysis of geomechanical parameters”. *European Journal of Environmental and Civil Engineering*, 20(1), 2016, pp. 60-78.
13. Janin, J. P., Dias, D., Emeriault, F., Kastner, R., Le Bissonnais, H., Guilloux, A., “Numerical back-analysis of the southern Toulon tunnel measurements: a comparison of 3D and 2D approaches”. *Engineering Geology,* 195, 2015, pp. 42-52.
14. Tarifard, A., Görög, P., Török, Á., “Long-term assessment of creep and water effects on tunnel lining loads in weak rocks using displacement-based direct back analysis: an example from northwest of Iran”. *Geomechanics and Geophysics for Geo-Energy and Geo-Resources,* 8(1), 2022, pp. 1-15.
15. Wang, J. X., Sun, J., Kou, H. J., Lin, Y. X., Zhang, Z. T., “Multiparameter Inversion Early Warning System of Tunnel Stress-Seepage Coupling Based on IA-BP Algorithm”. *Advances in Civil Engineering*, 2021, 2021, pp. 1566693.
16. Lee, J. K., Yoo, H., Ban, H., Park, W. J., “Estimation of Rock Load of Multi-Arch Tunnel with Cracks Using Stress Variable Method”. *Applied Sciences*, 10(9), 2020, pp. 3285.
17. Mahmoudi, M., Rajabi, A. M., “Application of numerical back analysis for determination of soil mass specifications during tunnel construction”. *Arabian Journal of Geosciences*, 13(19), 2020, pp. 1-9.
18. Yu, J., Zhang, Q., Xu, W. Y., Wang, R. B., Zhang, H., “Study on unloading relaxation characteristics of columnar jointed rock mass based on displacement back analysis”. *Frontiers in Earth Science*, 9, 2021, pp. 779537.
19. An, J. S., Song, K. I., “Back analysis of an operating subsea tunnel considering the degradation of ground and concrete lining”. *Marine Georesources & Geotechnology*, 37(4), 2019, *pp. 517-523.*

20. Ghorbani, E., Moosavi, M., Hossaini, M. F., Assary, M., Golabchi, Y., "Determination of initial stress state and rock mass deformation modulus at Lavarak HEPP by back analysis using ant colony optimization and multivariable regression analysis". *Bulletin of Engineering Geology and the Environment*, 80(1), 2021, *pp. 429-442*.
21. Wang, X. Y., Shao, Z. S., "Theoretical Research on the Inverse Analysis of the Internal Force of the Primary Support in a Horseshoe Tunnel". *Modern Tunnelling Technology*, 51(6), 2014, pp. 83-88.
22. Cheng, Y. X., Cui, G. Q., Song, L., "Theoretical study on inversion analysis of internal force of support structure in multi-circle arc tunnel". *Modern Tunnelling Technology*, 55(1), 2018, pp. 85-89.
23. He, W. Z., Xu, L. S., Wang, L. L., "Theoretical Back Analysis of Internal Forces of Primary Support in Deep Tunnels". *Journal of Engineering Science & Technology Review*, 12(1), 2019, pp. 18-26.